

Article

Prognostic Immune Effector Signature in Adult Acute Lymphoblastic Leukemia Patients Is Dominated by $\gamma\delta$ T Cells

Anne-Charlotte Le Floch ^{1,2}, Marie-Sarah Rouvière ^{1,2}, Nassim Salem ^{1,2}, Amira Ben Amara ^{1,2},
Florence Orlanducci ^{1,2}, Norbert Vey ³, Laurent Gorvel ^{1,2}, Anne-Sophie Chretien ^{1,2} and Daniel Olive ^{1,2,*}

¹ Equipe Immunité et Cancer, Centre de Recherche en Cancérologie de Marseille (CRCM), INSERM U1068, CNRS UMR7258, Institut Paoli-Calmettes, Aix-Marseille Université, UM 105, 13009 Marseille, France; leflocha@ipc.unicancer.fr (A.-C.L.F.)

² Plateforme d'Immunomonitoring, Institut Paoli-Calmettes, 13009 Marseille, France

³ Département d'Hématologie, CRCM, INSERM U1068, CNRS UMR7258, Institut Paoli-Calmettes, Aix-Marseille Université, UM 105, 13009 Marseille, France

* Correspondence: daniel.olive@inserm.fr

Abstract: The success of immunotherapy has highlighted the critical role of the immune microenvironment in acute lymphoblastic leukemia (ALL); however, the immune landscape in ALL remains incompletely understood and most studies have focused on conventional T cells or NK cells. This study investigated the prognostic impact of circulating $\gamma\delta$ T-cell alterations using high-dimensional analysis in a cohort of newly diagnosed adult ALL patients (10 B-ALL; 9 Philadelphia⁺ ALL; 9 T-ALL). Our analysis revealed common alterations in CD8⁺ T cells and $\gamma\delta$ T cells of relapsed patients, including accumulation of early stage differentiation and increased expression of BTLA and CD73. We demonstrated that the circulating $\gamma\delta$ T-cell signature was the most discriminating between relapsed and disease-free groups. In addition, V δ 2 T-cell alterations strongly discriminated patients by relapse status. Taken together, these data highlight the role of $\gamma\delta$ T cells in adult ALL patients, among whom V δ 2 T cells may be a pivotal contributor to T-cell immunity in ALL. Our findings provide a strong rationale for further monitoring and potentiating V δ 2 T cells in ALL, including in the autologous setting.

Keywords: acute lymphoblastic leukemia; $\gamma\delta$ T cells; V δ 2 T cells; prognosis



Citation: Le Floch, A.-C.; Rouvière, M.-S.; Salem, N.; Ben Amara, A.; Orlanducci, F.; Vey, N.; Gorvel, L.; Chretien, A.-S.; Olive, D. Prognostic Immune Effector Signature in Adult Acute Lymphoblastic Leukemia Patients Is Dominated by $\gamma\delta$ T Cells. *Cells* **2023**, *12*, 1693. <https://doi.org/10.3390/cells12131693>

Academic Editors: Dieter Kabelitz and Loretta Tuosto

Received: 26 March 2023

Revised: 7 June 2023

Accepted: 14 June 2023

Published: 22 June 2023



Copyright: © 2023 by the authors. Licensee MDPI, Basel, Switzerland. This article is an open access article distributed under the terms and conditions of the Creative Commons Attribution (CC BY) license (<https://creativecommons.org/licenses/by/4.0/>).

1. Introduction

The success of immunotherapy in acute lymphoblastic leukemia (ALL) has highlighted the critical role of the immune microenvironment in this disease [1,2]. Despite the advances in allogeneic hematopoietic stem cell transplantation (HSCT) and the use of immunotherapeutic approaches such as monoclonal antibodies and CAR T-cell therapy [3], most adult patients with ALL relapse [4,5]. Before the age of 55 years, overall survival (OS) rates range from 50 to 60%, while survival in older patients does not exceed 30% [6].

ALL are heterogeneous entities arising from B-cell (B-ALL) or T-cell (T-ALL) precursors. B-ALL accounts for approximately 75% of ALL cases. Of these, 25–30% harbor the BCR-ABL1 fusion protein, which is the driver mutation of Philadelphia chromosome-positive acute lymphoblastic leukemia (Ph⁺-ALL). The prognosis of ALL is influenced by disease-related factors (central nervous system involvement, white blood cell count, cytogenetic and molecular subtype) and quality of response to treatment (MRD; Minimal Residual Disease), which are currently used for risk stratification and therapeutic decision making [3]. Although immunotherapeutic approaches predominate in ALL, immune changes remain poorly understood. Indeed, some studies have focused on cellular immune escape in ALL, demonstrating immunosuppressive functions of myeloid-derived infiltrating cells such as mesenchymal stromal cells (MSCs) [7], myeloid-derived suppressor cells (MDSCs) [8], and

tumor-associated macrophages (TAMs) [9], or the antitumor role of non-classical monocytes [10]. Conversely, the contribution of effector immune cells has been less studied in ALL. Cytotoxic T lymphocyte (CTL) and natural killer (NK) cell infiltration show defective activation and function [11–13]. This poor immunogenic response has been proposed to be related to the low mutational burden in ALL [2], qualitative or quantitative defects in HLA expression [14], and an imbalance in the expression of co-stimulatory or inhibitory molecules (PD-1/PDL-1 pathway, CTLA-4, or TIM-3) [15–17]. Immune escape in ALL is also mediated by regulatory T cells (T-regs) [18] and their frequency has been correlated with response to immunotherapies [19,20].

Most immunomonitoring studies of immune effectors in ALL have so far focused on conventional T cells or NK cells but data on $\gamma\delta$ T-cell populations are currently scarce. The crucial role of $\gamma\delta$ T cells in antimicrobial and antitumoral immunity has recently been demonstrated [21]. In contrast to MHC-restricted $\alpha\beta$ T cells [22], $\gamma\delta$ T-cell activation is mediated by ligand recognition by both TCR and non-TCR receptors such as DNAM-1 [23] or NKG2D [24]. $\gamma\delta$ T cells also represent a major discovery at the interface of innate and adaptive immunity [25,26]. In addition to their unique recognition mechanism, which remains partially identified, $\gamma\delta$ T cells could mediate a rapid and potent cytotoxic response [27]. They can activate $\alpha\beta$ T cells and invariant natural killer T cells and interact with NK cells, dendritic cells (DCs), macrophages, and neutrophils [28]. These properties make $\gamma\delta$ T cells prime candidates for cancer immunotherapy [29,30]. Human $\gamma\delta$ T cells represent 5–10% of circulating lymphocytes [31]. They can be classified into four groups based on the TCR δ -chain (V δ 1, V δ 2, V δ 3, and V δ 5) [32]. Human $\gamma\delta$ T cells in tissues and peripheral blood are predominantly composed of V δ 1 and V δ 2 T cells. Both exhibit pleiotropic antitumoral responses but also have specific characteristics that depend on the cancer subtype [33,34]. V δ 2 T cells are the major blood $\gamma\delta$ T-cell subtype and their activation is mediated by the recognition of non-peptidic phosphorylated metabolites that bind to butyrophilin 3A1 and 2A1 molecules [35–38].

In ALL, preliminary *in vitro* studies have shown that $\gamma\delta$ T cells exert potent cytotoxic functions against primary ALL blasts [39–42]. *In vivo* experiments have confirmed the activity of $\gamma\delta$ T cells in a xenogeneic CML model [43] and in a Ph⁺ ALL model [44]. $\gamma\delta$ T-cell-based immunotherapy after HSCT has also shown promising results. Indeed, an increased frequency of $\gamma\delta$ T cells in ALL patients undergoing $\alpha\beta$ -depleted HSCT was associated with improved OS [45–47]. In addition, *in vivo* stimulation of V δ 2 T cells with zoledronate (ZOL) after haploidentical HSCT improved outcomes in pediatric ALL patients [48]. Several clinical trials are currently investigating $\gamma\delta$ T-cell-based therapeutic approaches in various malignancies but few include ALL patients and only in the allogeneic setting [49]. Similarly, the prognostic role of $\gamma\delta$ T cells in adult ALL has mainly been studied after HSCT, where a better reconstitution of $\gamma\delta$ T cells was associated with a lower risk of relapse [45,46]. The role of $\gamma\delta$ T cells at diagnosis of adult ALL is based only on bulk transcriptome inference, which showed that higher TCRV δ 2⁺ $\gamma\delta$ TILs (tumor-infiltrating lymphocytes) were associated with prolonged survival [50]. Qualitative changes in $\gamma\delta$ T cells at diagnosis have only been investigated in small pediatric cohort studies of B-ALL, which showed that increased CTLA-4 and decreased CD8 expression on $\gamma\delta$ T cells were associated with poor outcomes [51,52]. Importantly, most studies of $\gamma\delta$ T cells in ALL have not distinguished between V δ 1 and V δ 2 subsets.

To date, no study has accurately described $\gamma\delta$ T-cell subsets and their changes at diagnosis in adult ALL patients and analyzed their correlation with outcomes.

This study aims to investigate the prognostic impact of the $\gamma\delta$ T-cell immunophenotype using high-dimensional analysis in a cohort of newly diagnosed treatment-naïve adult ALL patients. We mapped the peripheral gamma delta landscape by mass cytometry and determined the individual prognostic signature of V δ 1 and V δ 2 T cells.

2. Materials and Methods

2.1. Clinical Samples

Heparinized blood from 28 ALL patients were obtained before induction chemotherapy (10 B-ALL; 9 T-ALL; 9 Ph⁺ ALL), from the Department of Hematology of the Institute Paoli–Calmettes. Informed consent was obtained from all donors in accordance with the Declaration of Helsinki, and the study was approved by our Institutional Review Board (BTN-LAL-IPC2021-049—Immunomodulation dans les leucémies aiguës—22 June 2021). Baseline characteristics of the ALL patients are shown in Supplementary Table S1. Patients were diagnosed between May 2005 and March 2019 and were aged from 18 to 80 years old. All patients were treated with conventional induction chemotherapy.

Samples with more than 70% of blasts were selected for the study.

2.2. Flow and Mass Cytometry

For flow cytometry, PBMCs were washed and incubated with human Fc Block (BD Biosciences, San Jose, CA, USA) for 10 min at 4 °C before immunostaining with a mix of extracellular antibodies. Acquisition was performed on a BD FACS CANTO II (BD Biosciences) and data were analyzed using DIVA 8.0.1. The mass cytometry experiments were performed as previously described [53]. Briefly, PBMCs were washed with RPMI 1640 medium supplemented with 10% fetal calf serum (FCS) and incubated for 1 h at 37 °C with 5% CO₂ in RPMI 1640 with 2% FCS; Pierce Universal Nuclease 2.5 kU (Thermo Fisher Scientific, Waltham, MA, USA) was added in the last 30 min. The cells were centrifuged and incubated with cisplatin 5 µM to stain dead cells and then incubated with human Fc Block (BD Biosciences). A total of 1- to 2-million PBMCs were stained with the extracellular antibodies for 1 h at 4 °C (Supplementary Table S2, upper part). After centrifugation, the cells were washed and permeabilized with the Fixation/Transcription Factor Staining Buffer Set (eBioscience, San Diego, CA, USA) for 30 min at 4 °C. Cells were then preincubated with human Fc Block for 10 min at 4 °C before incubation with intracellular antibodies for 30 min at 4 °C (Supplementary Table S2, lower part). The cells were then washed and labeled overnight with 125 µM of DNA intercalator diluted in 2% PFA (Fluidigm–Standard Biotools, San Francisco, CA, USA). Finally, cells were diluted in EQ™ Four Element Calibration Beads (Fluidigm) and were acquired on a Helios mass cytometer (Fluidigm). After data acquisition, cells were further analyzed using FlowJo v10.6.2 (BD Biosciences) and OMIQ software from Dotmatics (accessed on 12 January 2023; www.omiq.ai, www.dotmatics.com).

2.3. Uniform Manifold Approximation and Projection Analysis

The uniform manifold approximation and projection (UMAP) dimensionality-reduction technique was used for immune subset identification and was performed using the OMIQ software from Dotmatics. Leukemic cells and immune subsets were identified according to the gating strategy shown in Supplementary Figure S1. BGA and statistical analyses were performed when all immune cell subsets contained more than 30 cells. Hierarchical clustering (Euclidean distance) and heat map visualization were performed using Phantasus v1.19.3.

2.4. Generation of Anti-Human BTN3A mAb

To generate anti-BTN3A 20.1, BALB/c mice were immunized with a soluble BT3.1-Ig fusion protein, as previously described [54].

2.5. Expansion of Vδ2 T Cells

PBMCs from ALL patients and HV (healthy volunteers) were isolated by density gradient (Lymphoprep) and were then frozen until use. To expand autologous Vδ2 T cells, frozen PBMCs from ALL patients were stimulated with ZOL 1 µM (Sigma-Aldrich, Saint Louis, MO) and rhIL-2 (Miltenyi Biotec, Bergisch Gladbach, Germany) at day 0. From day (d) 5, rhIL-2 was renewed every 2 days and the cells were maintained at 1.5×10^6 /mL

until d14. rhIL-15 (10 ng/mL; Miltenyi Biotec) was also added starting at d2 and was renewed every 2 days, as IL-15 has been shown to enhance the proliferative capacity of V δ 2 T cells [55–57]. Fresh autologous expanded V δ 2 T cells were then used for functional assays, depending on the quantity of V δ 2 T cells. The fold increase in viable V δ 2 T cells was calculated using the formula: (d14 %V δ 2 \times d14 total cell number)/(d0 % V δ 2 \times d0 total cell number).

2.6. Degranulation Assays

To analyze CD107 expression, fresh autologous V δ 2 T cells and primary ALL blasts were cocultured at an Effector:Target (E:T) ratio of 1:1 with anti-CD107a, anti-CD107b, Golgi stop, and anti-BTN3A 20.1 agonist mAb or isotype control (1 μ g/mL). After 4 h, cells were collected and analyzed by flow cytometry. Cells were acquired on a BD FACS CANTO II and analyzed using DIVA 8.0.1.

2.7. Statistics

Data were analyzed using between-group analysis (BGA). Variables with a mean frequency expression of less than 5% were excluded to avoid any assessment of background noise. The BGA was performed using RStudio v2022.07.2 (made4 package). R scripts used in the BGA are provided in Supplementary File S1.

Statistical analyses were performed using Graph Pad Prism 5.0 (Graph Pad Software, San Diego, CA, USA).

Normality of distributions was assessed using the D'Agostino–Pearson normality test.

Comparisons of continuous variables between two groups were performed using a two-tailed Mann–Whitney U test. The Kruskal–Wallis test followed by Dunn's post hoc test was used for multiple comparisons of independent samples.

3. Results

3.1. $\gamma\delta$ T-Cell Phenotypic Variables Are Significant Contributors to the Immune Effector Signature Associated with Relapse in ALL Patients

We first evaluated the global distribution of immune markers on circulating CD8⁺ T cells, NK cells, and $\gamma\delta$ T cells, of adult ALL patients at diagnosis and compared their respective contribution according to clinical outcomes. We analyzed peripheral blood mononuclear cells (PBMCs) by mass cytometry from 25 analyzable patients (9 B-ALL, 9 B-ALL Ph⁺, and 7 T-ALL) and quantified immune markers by manual gating (Supplementary Figure S1). This resulted in 89 variables that were analyzed by a between-group analysis (BGA) to generate a composite immune signature discriminating relapsed (REL) from disease-free (DF) ALL patients (n = 15 and n = 10, respectively) (Supplementary File S2). The BGA analysis provides the contribution of each immune variable and the relative contribution of each immune cell type to the discrimination of the groups compared. Of these 89 variables, 32, 28, and 29 were related to $\gamma\delta$ T cells, CD8⁺ T cells, and NK cells, respectively; therefore, the random theoretical relative contribution of each immune cell subset to group discrimination was 35.9%, 31.5%, and 32.6%, respectively. Figure 1A shows the result projection of all samples from the BGA analysis. The relative contribution of each variable according to the immune cell subtype is shown in Figure 1B. Variables associated with $\gamma\delta$ T cells contributed the most to the global discrimination (43.3%), followed by CD8⁺ T cells (33.2%), and NK cells (23.5%). By subtracting the expected contribution from the total contribution, we found that $\gamma\delta$ T-cell variables contributed +7.4% more than expected to the discrimination of groups, versus +1.7% for CD8⁺ T cells, and −9.1% for NK cell variables (Figure 1C).

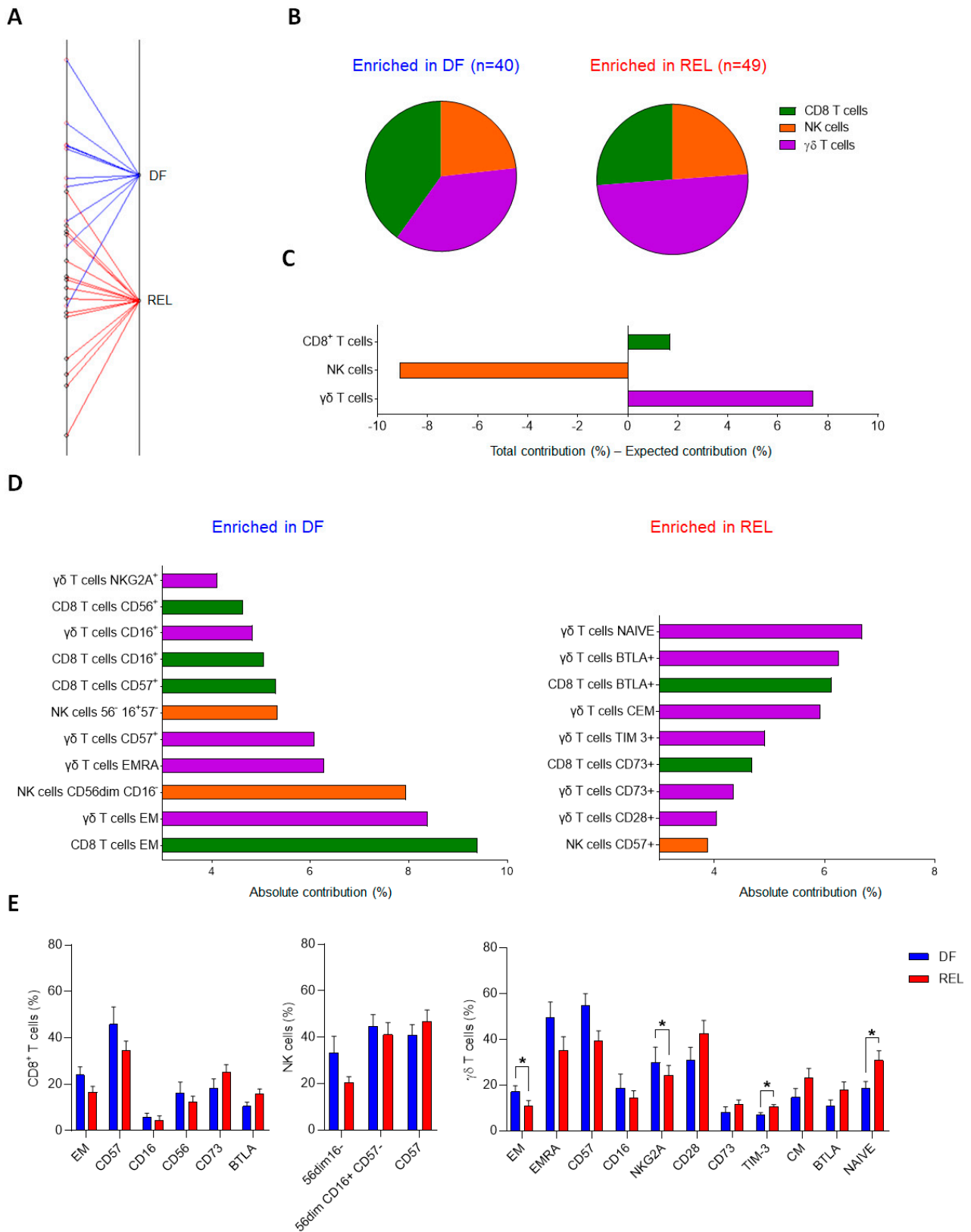


Figure 1. $\gamma\delta$ T-cell phenotypic variables are significant contributors to the immune effector signature associated with relapse in ALL patients. Results of between-group analysis (BGA) using 89 variables associated with CD8⁺ T cells (n = 28), NK cells (n = 29), or $\gamma\delta$ T cells (n = 32) from PBMCs of 9 B-ALL,

9 B-ALL Ph⁺, and 7 T-ALL patients are shown. (A) The axis shows the projection of all samples (n = 25). Sample origins from disease-free (DF) ALL patients (n = 10) are annotated in red; sample origins from relapsed (REL) ALL patients (n = 15) are annotated in black. Each sample origin is linked to its own group (blue trait for DF group; red trait for REL group). The degree of discrimination between groups and samples is given by the distances between group origins and the distances between sample origins, respectively. (B) The pie chart displays the respective contribution of the variables related to CD8⁺ T cells, NK cells, and $\gamma\delta$ T cells, to the discrimination of the DF group (blue) from the REL group (red). (C) The bar graph, whose Y-axis shows the difference between the total contribution and the expected contribution of each population to the discrimination of the DF group from the REL group. (D) The contribution of the top 20 discriminating immune variables from the BGA. The variables enriched in DF patients are shown in the left panel and the variables enriched in REL patients are shown in the right panel. (E) Frequency comparison of the top 20 circulating immune variables discriminating REL vs. DF groups. Comparison of immune cell variables of CD8⁺ T cells and NK cells from 10 B-ALL, 9 B-ALL Ph⁺, and 9 T-ALL patients, between DF group and REL group (DF, n = 11; REL n = 17). Comparison of immune cell variables of $\gamma\delta$ T cells from PBMCs of 9 B-ALL, 9 B-ALL Ph⁺, and 7 T-ALL patients, between DF group and REL group (DF, n = 10; REL, n = 15). Data are expressed as mean \pm standard error of the mean (SEM) (E). The statistical significance was established using a Mann–Whitney test. * $p < 0.05$ (E).

Consistently, analysis of the 20 most discriminating variables revealed 11, 6, and 3 immune variables associated with $\gamma\delta$ T cells, CD8⁺ T cells, and NK cells, respectively (Figure 1D). Variables associated with the differentiation and polarization states of both CD8⁺ T cells and $\gamma\delta$ T cells were the most differentially enriched; thus, the frequencies of effector memory (EM) CD8⁺ T cells and EM or EMRA (effector memory T cells re-expressing CD45RA) $\gamma\delta$ T cells were enriched in the DF group, whereas naive and CM $\gamma\delta$ T cells were enriched in the REL group. Consistently, DF patients had increased cytotoxic and priming markers on CD8⁺ T cells (CD16⁺, CD56⁺) and $\gamma\delta$ T cells (CD16⁺, CD57⁺, NKG2A⁺). In addition, some inhibitory or regulatory molecules were upregulated in the REL group: BTLA and CD73 on both CD8⁺ T cells and $\gamma\delta$ T cells, and TIM-3 on $\gamma\delta$ T cells. In contrast, the DF group was enriched for less mature NK cell subsets (CD56^{dim} CD16⁻ and CD56^{dim} CD16⁺CD57⁻), whereas highly differentiated NK cells (CD57⁺) were found in the REL group. Comparison of the frequencies of the 20 most discriminating variables revealed a significant difference between DF and REL patients only for the $\gamma\delta$ T-cell variables; REL patients had increased naive $\gamma\delta$ T cells, whereas DF patients had increased frequencies of EM $\gamma\delta$ T cells and NKG2A⁺ $\gamma\delta$ T cells (Figure 1E).

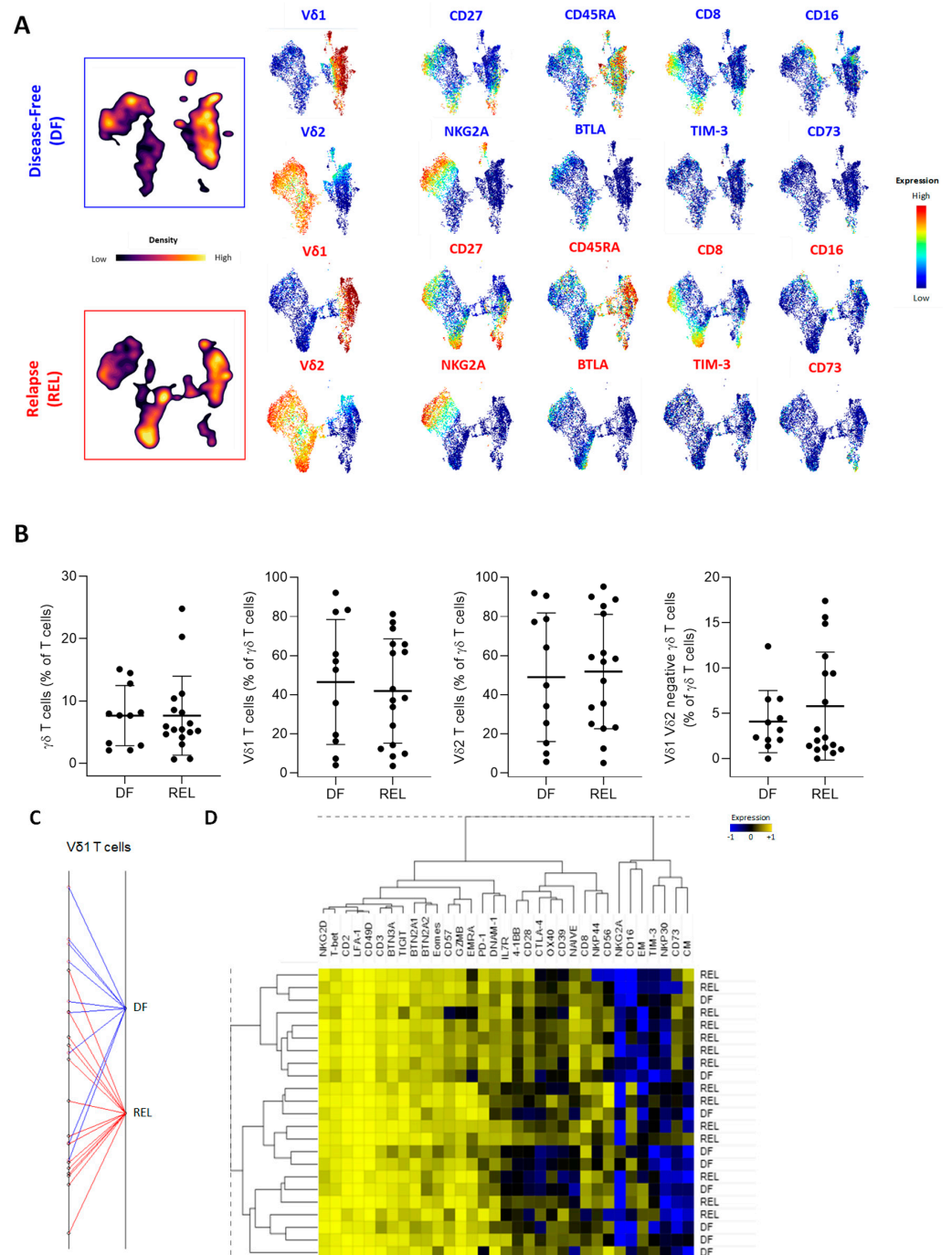
We also examined the differences in immune subsets according to ALL subtype; compared to HV, B-ALL patients had a lower frequency of monocytes. Conversely, T-ALL patients had a higher frequency of B-cells (Supplementary Figure S2). Regarding ICI expression, ALL patients showed high heterogeneity with a global trend towards higher ICI levels in REL patients (Supplementary Figure S3A). TIM-3 was significantly upregulated on $\gamma\delta$ T cells from REL patients and tended to be more expressed on CD8⁺ T cells and NK cells. A trend for other ICI upregulation was observed in REL patients, such as TIGIT on NK cells and BTLA and PD-1⁺ on $\gamma\delta$ T cells and CD8⁺ T cells.

This BGA of circulating immune effector markers in 25 ALL patients revealed common immune alterations in both CD8⁺ T cells and $\gamma\delta$ T cells and demonstrated that the circulating $\gamma\delta$ T-cell signature was the most discriminant between relapsed and disease-free groups. These results raise the question of the respective contribution of the two most abundant circulating $\gamma\delta$ T-cell populations: the V δ 1 and the V δ 2 subsets.

3.2. Prognostic Impact of $\gamma\delta$ T-Cell Alterations in ALL Mainly Depends on V δ 2 T Cells

Next, we compared the different $\gamma\delta$ T-cell subsets according to the occurrence of relapse. Figure 2 shows the results of UMAP analysis on $\gamma\delta$ T cells from all ALL patients. Analysis of the density of the $\gamma\delta$ T-cell subpopulations in each group (Figure 2A, left panel) showed marked differences in both V δ 1 and V δ 2 T-cell subsets but the frequency of $\gamma\delta$ T cells among lymphocytes was not different between DF and REL patients. The frequencies

of Vδ1 T cells, Vδ2 T cells, and of $\gamma\delta^+ V\delta2^- V\delta1^-$ T cells among $\gamma\delta$ T cells were also similar (Figure 2B). We further investigated the expression of the most discriminating variables associated with $\gamma\delta$ T cells according to our previous BGA analysis (Figure 2A, right panel).



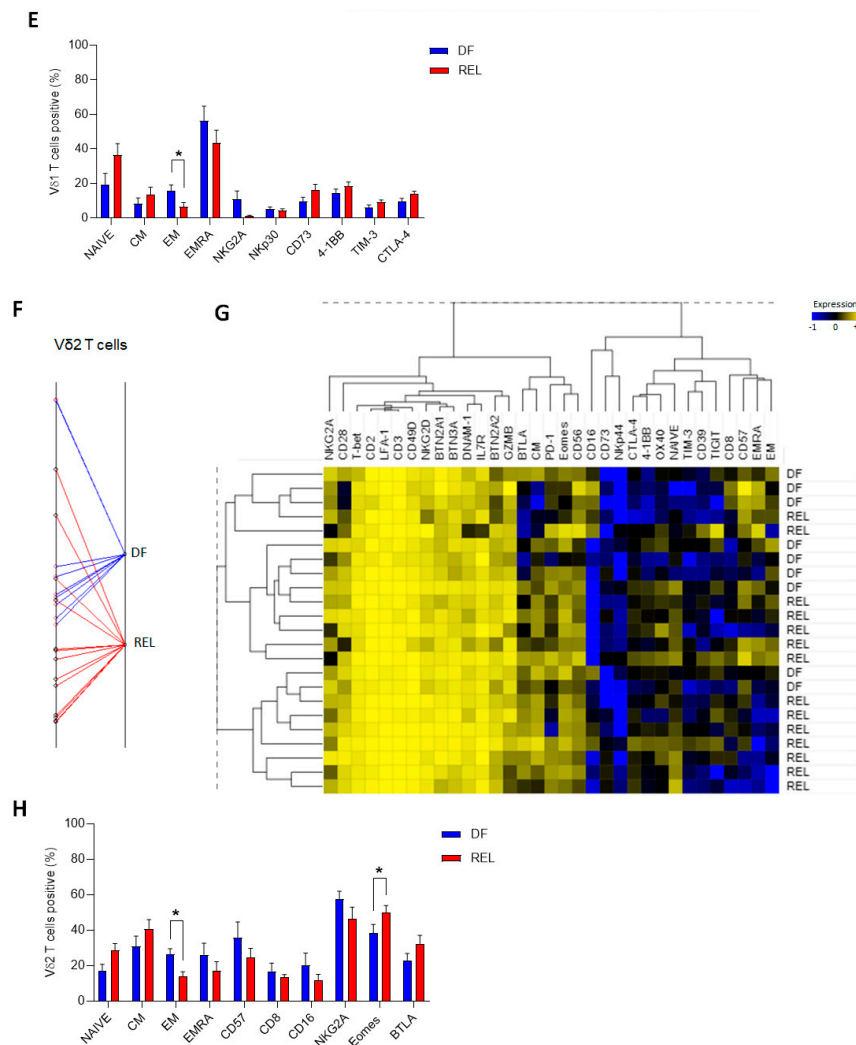


Figure 2. Prognostic impact of $\gamma\delta$ T-cell alterations in ALL mainly depends on V δ 2 T cells. (A) Peripheral blood $\gamma\delta$ T cells from ALL patients were manually gated, and consensus files were generated using the uniform manifold approximation and projection (UMAP) technique, with 5500 $\gamma\delta$ T cells for each group (DF, REL). In the left panel, the density of $\gamma\delta$ T-cell subpopulations in each patient group is projected (purple, low cell density; yellow, high cell density). Expression of markers of $\gamma\delta$ T-cell maturation, cytotoxicity, costimulation, and coinhibition are projected on UMAP maps in the right panel (blue, low expression; red, high expression). (B) The proportion of $\gamma\delta$ T cells among total T cells and the proportion of V δ 1⁺, V δ 2⁺, and V δ 1⁻/V δ 2⁻ T cells among total $\gamma\delta$ T cells (%) according to relapse status. (C) The results of a BGA using 33 variables associated with V δ 1 T cells are shown. The axis displays the projection of all samples (n = 23). Sample origins from DF patients (n = 9) are annotated in red; sample origins from REL patients (n = 14) are annotated in black. Each sample origin is linked to its own group (blue trait for DF group; red trait for REL group). (D) Unsupervised hierarchical clustering of 33 V δ 1 T-cell variables used in BGA. (E) Top 10 discriminating V δ 1 T-cell variables from BGA analysis. (F) The results of a BGA using 33 variables associated with V δ 2 T cells are shown. The axis displays the projection of all samples (n = 23). Sample origins from DF patients (n = 9) are annotated in red; sample origins from REL patients (n = 14) are annotated in black. Each sample origin is linked to its own group (blue trait for DF group; red trait for REL group). (G) Unsupervised hierarchical clustering of 33 V δ 2 T-cell variables used in BGA. (H) Top 10 discriminating V δ 2 T-cell variables from BGA analysis. Data are expressed as mean \pm SEM. The statistical significance was established using a Mann–Whitney test (B,E,H). * *p* < 0.05.

Some UMAP changes were observed on V δ 1 T cells and V δ 2 T cells, such as a globally increased expression of CD27⁺ subsets in REL patients. In contrast, CD73 was expressed on V δ 1 T cells from REL patients and BTLA was predominantly expressed on V δ 2 T cells from REL patients (Supplementary Figure S3B). PhenoGraph clustering allowed the identification of 22 $\gamma\delta$ T-cell subpopulations, according to the co-expression of 32 $\gamma\delta$ T-cell variables (Supplementary Figure S4). Consistent with previous results, a pronounced heterogeneity of cluster repartition was observed; however, some clusters displayed a similar pattern regardless of the ALL subtype. Thus, an increased proportion of NKG2A⁺ V δ 1 T cells (cluster 9) and a decreased frequency of cluster 3 corresponding to CM V δ 2 T cells (CD27⁺, CD28⁺, CD45RA⁻) expressing low levels of cytotoxic markers and high levels of PD-1 and BTLA, were observed in the DF group. Both V δ 1 T cells and V δ 2 T cells showed phenotypic changes associated with relapse. We therefore further investigated their own contribution by performing a BGA (Supplementary File S3). The BGA of V δ 1 T-cell variables showed a clear sample dispersion (Figure 2C), which was more pronounced in the DF group. In contrast, most DF samples co-segregated in the BGA of V δ 2 T-cell variables (Figure 2F). Furthermore, non-hierarchical clustering (NHC) revealed that V δ 1 and V δ 2 T cells were segregated according to their differentiation state (Figure 2D,G). The naive population was associated with 4-1BB, OX-40, and CTLA-4 on both V δ 1 and V δ 2 T cells. In V δ 1 T cells, the EM population co-clustered with CD16 and NKG2A, and the EMRA population with GZMB and CD57, while frequencies of EM and EMRA V δ 2 T cells were associated with CD57 and CD8. In addition, the CM subset was associated with CD73 on V δ 1 T cells and with BTLA on V δ 2 T cells. Overall, the NHC of V δ 1 T-cell variables poorly discriminated patients by relapse status, whereas the NHC of V δ 2 T-cell variables identified distinct clusters of DF and REL patients.

Further analysis of the most discriminating V δ 1 and V δ 2 T-cell variables found in the BGA revealed a significantly increased frequency of EM subsets in both V δ 1 and V δ 2 T cells in DF patients (Figure 2E,H). In addition, V δ 1 T cells from the REL group tended to have decreased levels of NKp30 and increased levels of CD73, TIM-3, and CTLA-4. In contrast, V δ 2 T cells from REL patients had higher levels of Eomes and tended to have increased BTLA expression, fewer cytotoxic markers (CD8, CD16), and a lower expression of CD57 and NKG2A.

This comparative high-dimensional analysis of V δ 1 and V δ 2 T cells revealed similar characteristics of both subsets in REL patients, with a decreased frequency of the most differentiated subsets; however, V δ 1 and V δ 2 T cells also exhibited a distinct inhibitory and regulatory profile, including an increased frequency of CD73⁺ V δ 1 T cells and of BTLA⁺ V δ 2 T cells. Importantly, V δ 2 T-cell variables made an important contribution to the BGA analysis and a non-hierarchical method confirmed their association with prognosis. These findings suggest that within the $\gamma\delta$ T-cell population, phenotypic alterations in V δ 2 T cells help to discriminate patients who will relapse, and also suggest that these V δ 2 T cells may have reduced effector capacities. To this end, we next investigated the extent to which these phenotypic changes were associated with functional alterations.

3.3. V δ 2 T Cells from Relapsed Patients Expand and Are Able to Degranulate and to Produce Th1 Cytokines

The expansion capacities of V δ 2 T cells were then explored with respect to the relapse status. Using ZOL stimulation combined with IL-2 plus IL-15 for 14 days, V δ 2 T cells from PBMCs of 18 ALL patients at diagnosis were expanded. REL patients had similar expansion capacities compared to DF patients (Figure 3A). Some of the samples were functionally tested by measuring degranulation and Th1 cytokine production of V δ 2 T cells, which did not appear to be altered in samples from REL patients, either spontaneously (Figure 3B) or by targeting BTN3A with the 20.1 agonist monoclonal antibody (Figure 3C).

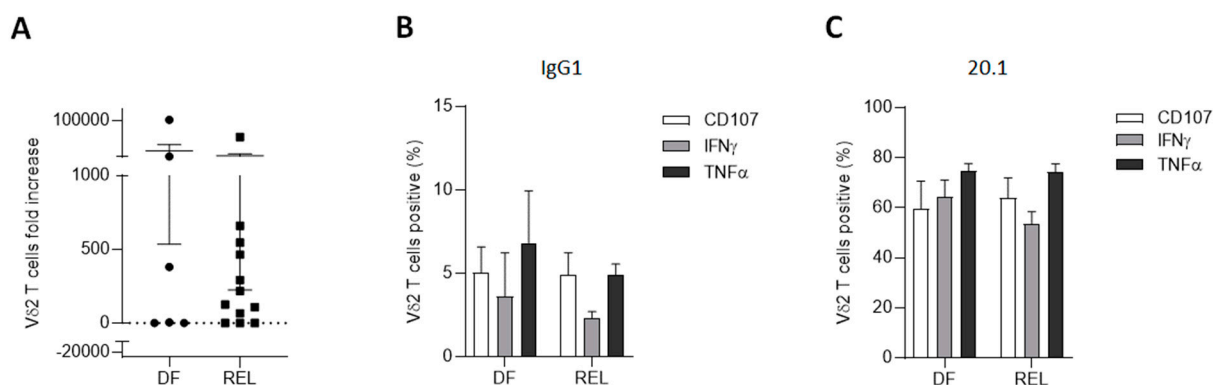


Figure 3. Vδ2 T cells from relapsed patients expand and are able to degranulate and produce Th1 cytokines. (A) PBMCs from ALL patients at diagnosis (n = 18; 6 DF and 12 REL patients) were cultured with ZOL for 14 days. (B,C) Effector functions of autologous expanded Vδ2 T cells (n = 4; 2 DF and 2 REL patients) were assessed after 4 h of co-culture with autologous primary ALL blasts (E:T ratio 1:1) in the presence of anti-BTN3A 20.1 (C) or its isotype control (B). Data are expressed as mean ± SEM. Statistical significance was determined by Mann–Whitney test (A).

This demonstrated, for the first time to our knowledge, that Vδ2 T cells from adult ALL patients were both able to expand in vitro after ZOL stimulation and to mediate cytotoxic activity against autologous blasts. It was also observed that the use of an anti-BTN3A agonist mAb enhanced the degranulation capacities of autologous Vδ2 T cells against primary ALL blasts, confirming results previously obtained only in primary AML samples [58].

Collectively, these results demonstrate that relapse-associated alterations in Vδ2 T cells do not affect either their proliferative or cytotoxic functions.

4. Discussion

While the prognostic value of $\gamma\delta$ T cells has been studied in adult ALL patients treated with HSCT, nothing was known about their potential impact at diagnosis. Here, we provide the first high-dimensional profiling of blood $\gamma\delta$ T cells in newly diagnosed adult ALL patients and show that their phenotypic changes discriminate patients according to clinical outcome. $\gamma\delta$ T cells are the most discriminant cytotoxic cell subtype and show common alterations regardless of ALL lineage; therefore, our results confirm previous studies on the prognostic impact of $\gamma\delta$ T cells in pediatric ALL patients [51,52], and provide a comprehensive analysis of Vδ1 and Vδ2 T-cell alterations in adult ALL patients.

The global immune effector signature between DF and REL patients identified major changes in conventional CD8⁺ T cells and $\gamma\delta$ T cells. Some were shared by both immune cells, including in DF patients, the expansion of late-stage CD8⁺ T cells and $\gamma\delta$ T cells, which was also associated with an increased expression of cytotoxic molecules, including CD16 on CD8⁺ T cells and $\gamma\delta$ T cells, and CD56 on CD8⁺ T cells. T-cell maturation stage has not yet been associated with prognosis in ALL patients but an increased infiltration of late-stage effector T cells was found in the BM of 100 B-ALL patients compared to HV [17]. In addition, CD8⁺ T cells and $\gamma\delta$ T cells from REL patients exhibited a globally immature and poorly cytotoxic profile, with increased levels of CD73 and BTLA. In contrast to the known immunosuppressive effect of CD73-adenosine signaling in solid tumors [59], there are no data on the CD73 expression on T cells in ALL; however, CD34⁺CD73⁺ blasts overexpress multidrug resistance markers such as BCL2, PGP, and MRP1 [60]. BTLA expression on TILs has been frequently associated with impaired anti-tumor T-cell responses in several cancer subtypes [61]. In large-cell lymphoma, BTLA⁺ T cells are less differentiated and have impaired killing capacity [62]. Regarding the impact of BTLA on $\gamma\delta$ T cells, BTLA limits the proliferation and the cytokine secretion of mature lymph node $\gamma\delta$ T cells [63], and our team has shown that BTLA decreases the proliferation of Vδ2 T cells and may also limit their differentiation [64]. In both adult AML and ALL, BTLA expression on

primary blasts correlates with poor outcomes [65,66]. In addition, genetic deletion of BTLA in a mouse model of ALL is associated with impaired blastic cell proliferation and colony formation [66]. Taken together, BTLA and CD73 expression on both blastic and immune cells may have a negative impact on ALL. Accordingly, it can be hypothesized that the ALL microenvironment may affect both leukemic and non-leukemic cells in the same way as has been demonstrated in T-ALL [67]. Indeed, our findings reinforce the need to better understand the regulation of these molecules during leukemogenesis and their role in immune evasion mechanisms. Regarding other ICI, TIM-3 tended to be overexpressed on all immune effectors studied. These results are consistent with the emerging role of this novel immunosenescence marker in ALL. TIM-3 inhibits CD8⁺ T-cell responses in early T-ALL [67], and higher numbers of TIM-3⁺/PD-1⁺ CD4⁺ T cells or TIM-3⁺ CD4⁺ T cells predict poor survival in adult B-ALL [15] and pediatric B-ALL [17]. In addition, TIM-3⁺ $\gamma\delta$ T cells have reduced killing capacity against colorectal cancer cells [68]. Furthermore, highly heterogeneous ICI expression was observed in our samples with a trend toward global upregulation. This is in line with previous studies showing a significant heterogeneity of PD-1, CTLA-4, or TIM-3 expression on CD8⁺ T cells in ALL patients compared to HV [15,17]. However, in contrast to BTLA and TIM-3, the prognostic contribution of other ICIs did not appear to be critical in our analysis. It can also be hypothesized that this heterogeneity reflects the diversity of our cohort; however, such heterogeneous signatures have been reported in both B-ALL [69] and T-ALL [70]. Indeed, analysis of $\gamma\delta$ T-cell clusters had shown that some cluster changes were restricted to one ALL lineage, these data were consistent with the discrepancies in the immune landscape observed in T-ALL and B-ALL [71] and suggest that this may also be true for $\gamma\delta$ T cells.

Our results showed that among circulating $\gamma\delta$ T cells, the V δ 2 T-cell signature associated with relapse was more discriminant. V δ 2 T cells from REL patients had a poorly differentiated profile with low cytotoxic markers and increased BTLA and Eomes levels. In CD8⁺ T cells, Eomes promotes the acquisition of cytotoxic potential [72] but is also involved in the control of T-cell exhaustion [73]. Although V δ 2 T cells are absent in rodents, it has been shown that $\gamma\delta$ T cells from mice expressing high levels of Eomes exhibit an exhausted phenotype and a reduced IFN- γ production [74]. Despite their marked alterations, V δ 2 T cells from REL patients were “activable”, as they were able to expand after ZOL treatment—similar to the DF ALL group—and mediate effector functions against autologous blasts. To date, the only $\gamma\delta$ T cells described to expand *in vitro* in ALL are V δ 1 T cells [42]. Previously, expansion of V δ 2 T cells from PBMCs of ITK-treated CML patients with BrHpp or ZOL has been reported, and these cells efficiently kill ZOL-sensitized autologous or allogeneic CML cells [43]. As in other malignancies with bone involvement, ZOL represents an emerging treatment in ALL [75] and its pleiotropic effects may also be based on ZOL-induced activation of V δ 2 T cells. Indeed, our results support the successful *in vivo* expansion of V δ 2 T cells from 46 pediatric ALL patients following ZOL administration after TcR $\alpha\beta$ /CD19-depleted haploidentical HSCT [48]. ZOL treatment resulted in the induction of both V δ 2 and V δ 1 T-cell subsets, with increased cytotoxicity of V δ 2 T cells against primary leukemia blasts [76].

Our study may have been limited by a small number of patients, and the effect of ICI expression on blood samples may not reflect the degree of T-cell exhaustion in the microenvironment. Tumor-infiltrating T cells are known to have a more exhausted phenotype than their circulating counterparts in both solid tumors [77,78] and in B-ALL after HSCT [14]; however, conflicting data have been reported for $\gamma\delta$ T cells in AML and in MM where no differences in checkpoint expression on V δ 1 and V δ 2 subsets have been observed [79]. Further studies are warranted to confirm our findings in a prospective manner and to compare the value of immune markers in the BM and peripheral compartments in ALL and their respective characteristics according to the ALL subtype. Furthermore, $\gamma\delta$ T cells are a major contributor to the efficacy of immune checkpoint blockade (ICB) in many cancers [80,81], reinforcing the importance of further investigating the impact of ICI on these immune effectors in ALL patients. Finally, ALL has been described to have the lowest

cytolytic value compared to other hematologic malignancies [71]; thus, the high killing potential of $\gamma\delta$ T cells combined with the observation of enriched cytotoxic subsets of $\gamma\delta$ T cells in ALL patients with a good prognosis highlights the key role that $\gamma\delta$ T cells may play.

5. Conclusions

Taken together, this high-dimensional analysis of phenotypic changes places $\gamma\delta$ T cells at the center of ALL effector immunity. Our focus on $\gamma\delta$ T cells has revealed that ALL patients with relapse have major $\gamma\delta$ T-cell alterations at diagnosis and has confirmed that V δ 2 T cells may be a key contributor to the prognosis of ALL. Our findings provide a strong rationale for further monitoring and potentiating V δ 2 T cells in ALL, including in the autologous setting.

Supplementary Materials: The following supporting information can be downloaded at: <https://www.mdpi.com/article/10.3390/cells12131693/s1>, Figure S1: Dimensionality-reduction analysis of PBMCs from HV and newly diagnosed ALL patients enables identification of non-leukemic cells; Figure S2: Comparative frequencies of circulating immune subsets in HV and ALL patients; Figure S3: Immune check-point expression on circulating immune effectors; Figure S4: V δ 1 and V δ 2 T-cell clusters have different repartition according to ALL lineage; Table S1: Patient, disease characteristics, and response to treatment; Table S2: Mass cytometry panels (extracellular antibodies and intracellular antibodies). File S1: BGA R scripts. File S2: BGA of $\gamma\delta$ T cells between DF vs. REL samples. File S3: BGA of V δ 1 and V δ 2 T cells between DF vs. REL samples.

Author Contributions: Conceptualization, A.-C.L.F., A.-S.C. and D.O. Investigation, A.-C.L.F., A.B.A., N.S., F.O., L.G. and M.-S.R. Resources, N.V. Writing—review and editing, A.-C.L.F., N.V. and D.O. Supervision, A.-S.C., N.V. and D.O. Funding acquisition, D.O. All authors have read and agreed to the published version of the manuscript.

Funding: A.-C.L.F. was funded by the Fondation pour la Recherche Médicale (grant DEA 40820) from November 2016 to October 2017 and the Poste d’Accueil INSERM from November 2019 to October 2021. The “Immunity and Cancer” team was labeled “FRM DEQ20180339209” (for D.O.). This work has been financially supported by the Institut National du Cancer (INCa) (Grant 2012-064/2019-038 to D.O. and A.T.), the Fondation de France (Grant 00076207 to A.-S.C.), the ITMO cancer (grant 2014-P032760 to A.-S.C.), the Sites de Recherche Intégrée sur le Cancer (SIRIC) Marseille (grant INCa-DGOS-INSERM 6038), and the Groupement d’intérêt scientifique -Infrastructures pour la Biologie, la Santé et l’Agriculture (GIS IBiSA), the Association Laurette Fugain (grant ALF2020/05 for D.O.), and the Agence Nationale de la Recherche [French National Infrastructure for Mouse Phenogenomics (PHENOMIN) project].

Institutional Review Board Statement: The study was approved by the local ethics board (BTN-LAL-IPC2021-049—Immunomodulation dans les leucémies aigües—22 June 2021).

Informed Consent Statement: Written informed consent was obtained from all patients.

Data Availability Statement: The datasets used and/or analyzed during the current study are available from the corresponding authors upon reasonable request (leflocha@ipc.unicancer.fr).

Acknowledgments: We thank the IPC Immunomonitoring platform and the IPC Tumor Bank (authorization number AC-2007-33), granted by the French Ministry of Research.

Conflicts of Interest: D.O. is a co-founder and shareholder of Imcheck Therapeutics and is currently a consultant to the company, which has no effect on the interpretation of the data. Other authors declare that the research was conducted in the absence of any commercial or financial relationships that could be construed as a potential conflict of interest.

References

1. Pastorczak, A.; Domka, K.; Fidy, K.; Poprzeczko, M.; Firczuk, M. Mechanisms of Immune Evasion in Acute Lymphoblastic Leukemia. *Cancers* **2021**, *13*, 1536. [[CrossRef](#)] [[PubMed](#)]
2. Jiménez-Morales, S.; Aranda-Urbe, I.S.; Pérez-Amado, C.J.; Ramírez-Bello, J.; Hidalgo-Miranda, A. Mechanisms of Immunosuppressive Tumor Evasion: Focus on Acute Lymphoblastic Leukemia. *Front. Immunol.* **2021**, *12*, 737340. [[CrossRef](#)] [[PubMed](#)]

3. Brown, P.A.; Shah, B.; Advani, A.; Aoun, P.; Boyer, M.W.; Burke, P.W.; DeAngelo, D.J.; Dinner, S.; Fathi, A.T.; Gauthier, J.; et al. Acute Lymphoblastic Leukemia, Version 2.2021, NCCN Clinical Practice Guidelines in Oncology. *J. Natl. Compr. Cancer Netw.* **2021**, *19*, 1079–1109. [[CrossRef](#)]
4. Sung, H.; Ferlay, J.; Siegel, R.L.; Laversanne, M.; Soerjomataram, I.; Jemal, A.; Bray, F. Global Cancer Statistics 2020: GLOBOCAN Estimates of Incidence and Mortality Worldwide for 36 Cancers in 185 Countries. *CA A Cancer J. Clin.* **2021**, *71*, 209–249. [[CrossRef](#)]
5. Sasaki, K.; Jabbour, E.; Short, N.J.; Jain, N.; Ravandi, F.; Pui, C.-H.; Kantarjian, H. Acute Lymphoblastic Leukemia: A Population-Based Study of Outcome in the United States Based on the Surveillance, Epidemiology, and End Results (SEER) Database, 1980–2017. *Am. J. Hematol.* **2021**, *96*, 650–658. [[CrossRef](#)] [[PubMed](#)]
6. Huguët, F.; Chevret, S.; Leguay, T.; Thomas, X.; Boissel, N.; Escoffre-Barbe, M.; Chevallier, P.; Hunault, M.; Vey, N.; Bonmati, C.; et al. Intensified Therapy of Acute Lymphoblastic Leukemia in Adults: Report of the Randomized GRAALL-2005 Clinical Trial. *J. Clin. Oncol.* **2018**, *36*, 2514–2523. [[CrossRef](#)] [[PubMed](#)]
7. Polak, R.; de Rooij, B.; Pieters, R.; den Boer, M.L. B-Cell Precursor Acute Lymphoblastic Leukemia Cells Use Tunneling Nanotubes to Orchestrate Their Microenvironment. *Blood* **2015**, *126*, 2404–2414. [[CrossRef](#)]
8. Liu, Y.-F.; Chen, Y.-Y.; He, Y.-Y.; Wang, J.-Y.; Yang, J.-P.; Zhong, S.-L.; Jiang, N.; Zhou, P.; Jiang, H.; Zhou, J. Expansion and Activation of Granulocytic, Myeloid-Derived Suppressor Cells in Childhood Precursor B Cell Acute Lymphoblastic Leukemia. *J. Leukoc. Biol.* **2017**, *102*, 449–458. [[CrossRef](#)]
9. Lyu, A.; Triplett, T.A.; Nam, S.H.; Hu, Z.; Arasappan, D.; Godfrey, W.H.; Ames, R.Y.; Sarang, A.; Selden, H.J.; Lee, C.-H.; et al. Tumor-Associated Myeloid Cells Provide Critical Support for T-ALL. *Blood* **2020**, *136*, 1837–1850. [[CrossRef](#)]
10. Witkowski, M.T.; Dolgalev, I.; Evensen, N.A.; Ma, C.; Chambers, T.; Roberts, K.G.; Sreeram, S.; Dai, Y.; Tikhonova, A.N.; Lasry, A.; et al. Extensive Remodeling of the Immune Microenvironment in B Cell Acute Lymphoblastic Leukemia. *Cancer Cell* **2020**, *37*, 867–882.e12. [[CrossRef](#)]
11. D’Amico, G.; Vulcano, M.; Bugarin, C.; Bianchi, G.; Pirovano, G.; Bonamino, M.; Marin, V.; Allavena, P.; Biagi, E.; Biondi, A. CD40 Activation of BCP-ALL Cells Generates IL-10-Producing, IL-12-Defective APCs That Induce Allogeneic T-Cell Anergy. *Blood* **2004**, *104*, 744–751. [[CrossRef](#)] [[PubMed](#)]
12. Feng, Y.-Y.; Griffith, O.L.; Griffith, M. Clinical Implications of Neopeptide Landscapes for Adult and Pediatric Cancers. *Genome Med.* **2017**, *9*, 77. [[CrossRef](#)] [[PubMed](#)]
13. Rouce, R.H.; Shaim, H.; Sekine, T.; Weber, G.; Ballard, B.; Ku, S.; Barese, C.; Murali, V.; Wu, M.-F.; Liu, H.; et al. The TGF- β /SMAD Pathway Is an Important Mechanism for NK Cell Immune Evasion in Childhood B-Acute Lymphoblastic Leukemia. *Leukemia* **2016**, *30*, 800–811. [[CrossRef](#)] [[PubMed](#)]
14. Liu, L.; Chang, Y.-J.; Xu, L.-P.; Zhang, X.-H.; Wang, Y.; Liu, K.-Y.; Huang, X.-J. T Cell Exhaustion Characterized by Compromised MHC Class I and II Restricted Cytotoxic Activity Associates with Acute B Lymphoblastic Leukemia Relapse after Allogeneic Hematopoietic Stem Cell Transplantation. *Clin. Immunol.* **2018**, *190*, 32–40. [[CrossRef](#)]
15. Hohtari, H.; Brück, O.; Blom, S.; Turkki, R.; Sinisalo, M.; Kovanen, P.E.; Kallioniemi, O.; Pellinen, T.; Porkka, K.; Mustjoki, S. Immune Cell Constitution in Bone Marrow Microenvironment Predicts Outcome in Adult ALL. *Leukemia* **2019**, *33*, 1570–1582. [[CrossRef](#)]
16. Mansour, A.; Elkhodary, T.; Darwish, A.; Mabed, M. Increased Expression of Costimulatory Molecules CD86 and SCTLA-4 in Patients with Acute Lymphoblastic Leukemia. *Leuk. Lymphoma* **2014**, *55*, 2120–2124. [[CrossRef](#)]
17. Blaeschke, F.; Willier, S.; Stenger, D.; Lepenies, M.; Horstmann, M.A.; Escherich, G.; Zimmermann, M.; Rojas Ringeling, F.; Canzar, S.; Kaeuferle, T.; et al. Leukemia-Induced Dysfunctional TIM-3+CD4+ Bone Marrow T Cells Increase Risk of Relapse in Pediatric B-Precursor ALL Patients. *Leukemia* **2020**, *34*, 2607–2620. [[CrossRef](#)]
18. Niedźwiecki, M.; Budziło, O.; Adamkiewicz-Drożyńska, E.; Pawlik-Gwozdecka, D.; Zieliński, M.; Maciejka-Kembłowska, L.; Szczepański, T.; Trzonkowski, P. CD4+CD25highCD127low/-FoxP3 + Regulatory T-Cell Population in Acute Leukemias: A Review of the Literature. *J. Immunol. Res.* **2019**, *2019*, 2816498. [[CrossRef](#)]
19. Duell, J.; Dittrich, M.; Bedke, T.; Mueller, T.; Eisele, F.; Rosenwald, A.; Rasche, L.; Hartmann, E.; Dandekar, T.; Einsele, H.; et al. Frequency of Regulatory T Cells Determines the Outcome of the T-Cell-Engaging Antibody Blinatumomab in Patients with B-Precursor ALL. *Leukemia* **2017**, *31*, 2181–2190. [[CrossRef](#)]
20. An, F.; Wang, H.; Liu, Z.; Wu, F.; Zhang, J.; Tao, Q.; Li, Y.; Shen, Y.; Ruan, Y.; Zhang, Q.; et al. Influence of Patient Characteristics on Chimeric Antigen Receptor T Cell Therapy in B-Cell Acute Lymphoblastic Leukemia. *Nat. Commun.* **2020**, *11*, 5928. [[CrossRef](#)]
21. Silva-Santos, B.; Mensurado, S.; Coffelt, S.B. $\Gamma\delta$ T Cells: Pleiotropic Immune Effectors with Therapeutic Potential in Cancer. *Nat. Rev. Cancer* **2019**, *19*, 392–404. [[CrossRef](#)]
22. Motulsky, A.G. The 1985 Nobel Prize in Physiology or Medicine. *Science* **1986**, *231*, 126–129. [[CrossRef](#)]
23. Iguchi-Manaka, A.; Kai, H.; Yamashita, Y.; Shibata, K.; Tahara-Hanaoka, S.; Honda, S.; Yasui, T.; Kikutani, H.; Shibuya, K.; Shibuya, A. Accelerated Tumor Growth in Mice Deficient in DNAM-1 Receptor. *J. Exp. Med.* **2008**, *205*, 2959–2964. [[CrossRef](#)]
24. Guerra, N.; Tan, Y.X.; Joncker, N.T.; Choy, A.; Gallardo, F.; Xiong, N.; Knoblaugh, S.; Cado, D.; Greenberg, N.R.; Raulet, D.H. NKG2D-Deficient Mice Are Defective in Tumor Surveillance in Models of Spontaneous Malignancy. *Immunity* **2008**, *28*, 571–580. [[CrossRef](#)] [[PubMed](#)]
25. Morandi, F.; Yazdanifar, M.; Cocco, C.; Bertaina, A.; Airoidi, I. Engineering the Bridge between Innate and Adaptive Immunity for Cancer Immunotherapy: Focus on $\Gamma\delta$ T and NK Cells. *Cells* **2020**, *9*, 1757. [[CrossRef](#)] [[PubMed](#)]

26. Holtmeier, W.; Kabelitz, D. $\Gamma\delta$ T Cells Link Innate and Adaptive Immune Responses. *Mech. Epithel. Def.* **2005**, *86*, 151–183. [[CrossRef](#)]
27. Gao, Y.; Yang, W.; Pan, M.; Scully, E.; Girardi, M.; Augenlicht, L.H.; Craft, J.; Yin, Z. $\Gamma\delta$ T Cells Provide an Early Source of Interferon γ in Tumor Immunity. *J. Exp. Med.* **2003**, *198*, 433–442. [[CrossRef](#)] [[PubMed](#)]
28. Chan, K.F.; Duarte, J.D.G.; Ostrouska, S.; Behren, A. $\Gamma\delta$ T Cells in the Tumor Microenvironment—Interactions with Other Immune Cells. *Front. Immunol.* **2022**, *13*, 894315. [[CrossRef](#)]
29. Yazdanifar, M.; Barbarito, G.; Bertaina, A.; Airoidi, I. $\Gamma\delta$ T Cells: The Ideal Tool for Cancer Immunotherapy. *Cells* **2020**, *9*, 1305. [[CrossRef](#)]
30. Kabelitz, D.; Serrano, R.; Kouakanou, L.; Peters, C.; Kalyan, S. Cancer Immunotherapy with $\Gamma\delta$ T Cells: Many Paths Ahead of Us. *Cell Mol. Immunol.* **2020**, *17*, 925–939. [[CrossRef](#)]
31. De Libero, G. Sentinel Function of Broadly Reactive Human $\Gamma\delta$ T Cells. *Immunol. Today* **1997**, *18*, 22–26. [[CrossRef](#)] [[PubMed](#)]
32. LeFranc, M.P.; Forster, A.; Baer, R.; Stinson, M.A.; Rabbitts, T.H. Diversity and Rearrangement of the Human T Cell Rearranging Gamma Genes: Nine Germ-Line Variable Genes Belonging to Two Subgroups. *Cell* **1986**, *45*, 237–246. [[CrossRef](#)]
33. Paul, S.; Lal, G. Regulatory and Effector Functions of Gamma-Delta ($\Gamma\delta$) T Cells and Their Therapeutic Potential in Adoptive Cellular Therapy for Cancer. *Int. J. Cancer* **2016**, *139*, 976–985. [[CrossRef](#)] [[PubMed](#)]
34. Zhao, Y.; Niu, C.; Cui, J. Gamma-Delta ($\Gamma\delta$) T Cells: Friend or Foe in Cancer Development? *J. Transl. Med.* **2018**, *16*, 3. [[CrossRef](#)]
35. Rigau, M.; Ostrouska, S.; Fulford, T.S.; Johnson, D.N.; Woods, K.; Ruan, Z.; McWilliam, H.E.G.; Hudson, C.; Tutuka, C.; Wheatley, A.K.; et al. Butyrophilin 2A1 Is Essential for Phosphoantigen Reactivity by $\Gamma\delta$ T Cells. *Science* **2020**, *367*, eaay5516. [[CrossRef](#)] [[PubMed](#)]
36. Karunakaran, M.M.; Willcox, C.R.; Salim, M.; Paletta, D.; Fichtner, A.S.; Noll, A.; Starick, L.; Nöhren, A.; Begley, C.R.; Berwick, K.A.; et al. Butyrophilin-2A1 Directly Binds Germline-Encoded Regions of the $V\gamma 9V\delta 2$ TCR and Is Essential for Phosphoantigen Sensing. *Immunity* **2020**, *52*, 487–498.e6. [[CrossRef](#)]
37. Cano, C.E.; Pasero, C.; De Gassart, A.; Kerneur, C.; Gabriac, M.; Fullana, M.; Granarolo, E.; Hoet, R.; Scotet, E.; Rafia, C.; et al. BTN2A1, an Immune Checkpoint Targeting $V\gamma 9V\delta 2$ T Cell Cytotoxicity against Malignant Cells. *Cell Rep.* **2021**, *36*, 109359. [[CrossRef](#)]
38. Yuan, L.; Ma, X.; Yang, Y.; Li, X.; Ma, W.; Yang, H.; Huang, J.-W.; Xue, J.; Yi, S.; Zhang, M.; et al. Phosphoantigens Are Molecular Glues That Promote Butyrophilin 3A1/2A1 Association Leading to $V\gamma 9V\delta 2$ T Cell Activation. *BioRxiv* **2022**, 2022.01.02.474068.
39. Duval, M.; Yotnda, P.; Bensussan, A.; Oudhiri, N.; Guidal, C.; Rohrllich, P.; Boumsell, L.; Grandchamp, B.; Vilmer, E. Potential Antileukemic Effect of Gamma Delta T Cells in Acute Lymphoblastic Leukemia. *Leukemia* **1995**, *9*, 863–868.
40. Lança, T.; Correia, D.V.; Moita, C.F.; Raquel, H.; Neves-Costa, A.; Ferreira, C.; Ramalho, J.S.; Barata, J.T.; Moita, L.F.; Gomes, A.Q.; et al. The MHC Class Ib Protein ULBP1 is a Nonredundant Determinant of Leukemia/Lymphoma Susceptibility to $\Gamma\delta$ T-Cell Cytotoxicity. *Blood* **2010**, *115*, 2407–2411. [[CrossRef](#)]
41. Gomes, A.Q.; Correia, D.V.; Grosso, A.R.; Lança, T.; Ferreira, C.; Lacerda, J.F.; Barata, J.T.; da Silva, M.G.; Silva-Santos, B. Identification of a Panel of Ten Cell Surface Protein Antigens Associated with Immunotargeting of Leukemias and Lymphomas by Peripheral Blood Gammadelta T Cells. *Haematologica* **2010**, *95*, 1397–1404. [[CrossRef](#)] [[PubMed](#)]
42. Lamb, L., Jr.; Musk, P.; Ye, Z.; van Rhee, F.; Geier, S.S.; Tong, J.-J.; King, K.M.; Henslee-Downey, P.J. Human $\Gamma\delta^+$ T Lymphocytes Have *in Vitro* Graft vs Leukemia Activity in the Absence of an Allogeneic Response. *Bone Marrow Transplant.* **2001**, *27*, 601–606. [[CrossRef](#)] [[PubMed](#)]
43. D’Asaro, M.; Mendola, C.L.; Liberto, D.D.; Orlando, V.; Todaro, M.; Spina, M.; Guggino, G.; Meraviglia, S.; Caccamo, N.; Messina, A.; et al. $V\gamma 9V\delta 2$ T Lymphocytes Efficiently Recognize and Kill Zoledronate-Sensitized, Imatinib-Sensitive, and Imatinib-Resistant Chronic Myelogenous Leukemia Cells. *J. Immunol.* **2010**, *184*, 3260–3268. [[CrossRef](#)] [[PubMed](#)]
44. Siegers, G.M.; Felizardo, T.C.; Mathieson, A.M.; Kosaka, Y.; Wang, X.-H.; Medin, J.A.; Keating, A. Anti-Leukemia Activity of *in Vitro*-Expanded Human Gamma Delta T Cells in a Xenogeneic Ph⁺ Leukemia Model. *PLoS ONE* **2011**, *6*, e16700. [[CrossRef](#)] [[PubMed](#)]
45. Lamb, L.S.; Henslee-Downey, P.J.; Parrish, R.S.; Godder, K.; Thompson, J.; Lee, C.; Gee, A.P. Increased Frequency of TCR Gamma Delta + T Cells in Disease-Free Survivors Following T Cell-Depleted, Partially Mismatched, Related Donor Bone Marrow Transplantation for Leukemia. *J. Hematother.* **1996**, *5*, 503–509. [[CrossRef](#)]
46. Godder, K.T.; Henslee-Downey, P.J.; Mehta, J.; Park, B.S.; Chiang, K.-Y.; Abhyankar, S.; Lamb, L.S. Long Term Disease-Free Survival in Acute Leukemia Patients Recovering with Increased $\Gamma\delta$ T Cells after Partially Mismatched Related Donor Bone Marrow Transplantation. *Bone Marrow Transpl.* **2007**, *39*, 751–757. [[CrossRef](#)]
47. Marks, D.I.; Clifton-Hadley, L.; Copland, M.; Hussain, J.; Menne, T.F.; McMillan, A.; Moorman, A.V.; Morley, N.; Okasha, D.; Patel, B.; et al. *In-Vivo* T-Cell Depleted Reduced-Intensity Conditioned Allogeneic Haematopoietic Stem-Cell Transplantation for Patients with Acute Lymphoblastic Leukaemia in First Remission: Results from the Prospective, Single-Arm Evaluation of the UKALL14 Trial. *Lancet Haematol.* **2022**, *9*, e276–e288. [[CrossRef](#)]
48. Merli, P.; Algeri, M.; Galaverna, F.; Milano, G.M.; Bertaina, V.; Biagini, S.; Girolami, E.; Palumbo, G.; Sinibaldi, M.; Becilli, M.; et al. Immune Modulation Properties of Zoledronic Acid on Tc $\gamma\delta$ T-Lymphocytes After Tc $\alpha\beta$ /CD19-Depleted Haploidentical Stem Cell Transplantation: An Analysis on 46 Pediatric Patients Affected by Acute Leukemia. *Front. Immunol.* **2020**, *11*, 699. [[CrossRef](#)]
49. Saura-Esteller, J.; de Jong, M.; King, L.A.; Ensing, E.; Winograd, B.; de Grijl, T.D.; Parren, P.W.H.I.; van der Vliet, H.J. Gamma Delta T-Cell Based Cancer Immunotherapy: Past-Present-Future. *Front. Immunol.* **2022**, *13*, 915837. [[CrossRef](#)]

50. Tosolini, M.; Pont, F.; Poupot, M.; Vergez, F.; Nicolau-Travers, M.-L.; Vermijlen, D.; Sarry, J.-E.; Dieli, F.; Fournié, J.-J. Assessment of Tumor-Infiltrating TCRV γ 9V δ 2 T δ Lymphocyte Abundance by Deconvolution of Human Cancers Microarrays. *Oncoimmunology* **2017**, *6*, e1284723. [[CrossRef](#)]
51. Kang, S.H.; Hwang, H.J.; Yoo, J.W.; Kim, H.; Choi, E.S.; Hwang, S.-H.; Cho, Y.-U.; Jang, S.; Park, C.-J.; Im, H.J.; et al. Expression of Immune Checkpoint Receptors on T-Cells and Their Ligands on Leukemia Blasts in Childhood Acute Leukemia. *Anticancer Res.* **2019**, *39*, 5531–5539. [[CrossRef](#)] [[PubMed](#)]
52. Pawlik-Gwozdecka, D.; Zieliński, M.; Sakowska, J.; Adamkiewicz-Drożyńska, E.; Trzonkowski, P.; Niedźwiecki, M. CD8+ T δ T Cells Correlate with Favorable Prognostic Factors in Childhood Acute Lymphoblastic Leukemia. *Arch. Med. Sci.* **2021**, *17*, 561–563. [[CrossRef](#)] [[PubMed](#)]
53. Ben Amara, A.; Rouviere, M.-S.; Fattori, S.; Wlosik, J.; Gregori, E.; Boucherit, N.; Bernard, P.-L.; Nunès, J.A.; Vey, N.; Luche, H.; et al. High-Throughput Mass Cytometry Staining for Deep Phenotyping of Human Natural Killer Cells. *STAR Protoc.* **2022**, *3*, 101768. [[CrossRef](#)] [[PubMed](#)]
54. Compte, E.; Pontarotti, P.; Collette, Y.; Lopez, M.; Olive, D. Frontline: Characterization of BT3 Molecules Belonging to the B7 Family Expressed on Immune Cells. *Eur. J. Immunol.* **2004**, *34*, 2089–2099. [[CrossRef](#)]
55. García, V.E.; Jullien, D.; Song, M.; Uyemura, K.; Shuai, K.; Morita, C.T.; Modlin, R.L. IL-15 Enhances the Response of Human Gamma Delta T Cells to Nonpeptide [Correction of Nonpeptide] Microbial Antigens. *J. Immunol.* **1998**, *160*, 4322–4329. [[CrossRef](#)]
56. Aehnlich, P.; Carnaz Simões, A.M.; Skadborg, S.K.; Holmen Olofsson, G.; thor Straten, P. Expansion With IL-15 Increases Cytotoxicity of V γ 9V δ 2 T Cells and Is Associated with Higher Levels of Cytotoxic Molecules and T-Bet. *Front. Immunol.* **2020**, *11*, 1868. [[CrossRef](#)] [[PubMed](#)]
57. Van Acker, H.H.; Anguille, S.; Willemen, Y.; Van den Bergh, J.M.; Berneman, Z.N.; Lion, E.; Smits, E.L.; Van Tendeloo, V.F. Interleukin-15 Enhances the Proliferation, Stimulatory Phenotype, and Antitumor Effector Functions of Human Gamma Delta T Cells. *J. Hematol. Oncol.* **2016**, *9*, 1–13. [[CrossRef](#)]
58. Benyamine, A.; Le Roy, A.; Mamessier, E.; Gertner-Dardenne, J.; Castanier, C.; Orlanducci, F.; Pouyet, L.; Goubard, A.; Collette, Y.; Vey, N.; et al. BTN3A Molecules Considerably Improve V γ 9V δ 2 T Cells-Based Immunotherapy in Acute Myeloid Leukemia. *Oncoimmunology* **2016**, *5*, e1146843. [[CrossRef](#)]
59. Kong, Y.; Jia, B.; Zhao, C.; Claxton, D.F.; Sharma, A.; Annageldiyev, C.; Fotos, J.S.; Zeng, H.; Paulson, R.F.; Prabhu, K.S.; et al. Downregulation of CD73 Associates with T Cell Exhaustion in AML Patients. *J. Hematol. Oncol.* **2019**, *12*, 40. [[CrossRef](#)]
60. Zhou, Y.; Tse, E.W.-C.; Leung, R.; Cheung, E.; Li, H.; Sun, H. Multiplex Single-Cell Analysis of Cancer Cells Enables Unbiased Uncovering Subsets Associated with Cancer Relapse: Heterogeneity of Multidrug Resistance in Precursor B-ALL. *ChemMedChem* **2021**, *17*, e202100638. [[CrossRef](#)]
61. Ning, Z.; Liu, K.; Xiong, H. Roles of BTLA in Immunity and Immune Disorders. *Front. Immunol.* **2021**, *12*, 654960. [[CrossRef](#)] [[PubMed](#)]
62. Quan, L.; Lan, X.; Meng, Y.; Guo, X.; Guo, Y.; Zhao, L.; Chen, X.; Liu, A. BTLA Marks a Less Cytotoxic T-Cell Subset in Diffuse Large B-Cell Lymphoma with High Expression of Checkpoints. *Exp. Hematol.* **2018**, *60*, 47–56.e1. [[CrossRef](#)] [[PubMed](#)]
63. Bekiaris, V.; Šedý, J.R.; Macauley, M.G.; Rhode-Kurnow, A.; Ware, C.F. The Inhibitory Receptor BTLA Controls T δ T Cell Homeostasis and Inflammatory Responses. *Immunity* **2013**, *39*, 1082–1094. [[CrossRef](#)] [[PubMed](#)]
64. Gertner-Dardenne, J.; Fauriat, C.; Orlanducci, F.; Thibault, M.-L.; Pastor, S.; Fitzgibbon, J.; Bouabdallah, R.; Xerri, L.; Olive, D. The Co-Receptor BTLA Negatively Regulates Human V γ 9V δ 2 T-Cell Proliferation: A Potential Way of Immune Escape for Lymphoma Cells. *Blood* **2013**, *122*, 922–931. [[CrossRef](#)] [[PubMed](#)]
65. Radwan, S.M.; Elleboudy, N.S.; Nabih, N.A.; El-kholy, A.; Kamal, A.M. The Prospective Prognostic Value of the Immune Checkpoint BTLA Expression in Adult Acute Myeloid Leukemia Patients. *Egypt. J. Med. Hum. Genet.* **2021**, *22*, 78. [[CrossRef](#)]
66. Geng, H.; Chen, Z.; Anderson, S.; Fraser, E.; Lu, M.; Lingjing, C.; Collins, C.; Markus, M.; Rubenstein, J.L. Expression of B and T Lymphocyte Attenuator (BTLA) Correlates with CNS Metastasis and Adverse Prognosis in Activated B-Cell Lymphoma and Acute Lymphoblastic Leukemia. *Blood* **2015**, *126*, 3900. [[CrossRef](#)]
67. Anand, P.; Guillaumet-Adkins, A.; Dimitrova, V.; Yun, H.; Drier, Y.; Sotudeh, N.; Rogers, A.; Ouseph, M.M.; Nair, M.; Potdar, S.; et al. Single-Cell RNA-Seq Reveals Developmental Plasticity with Coexisting Oncogenic States and Immune Evasion Programs in ETP-ALL. *Blood* **2021**, *137*, 2463–2480. [[CrossRef](#)]
68. Li, X.; Lu, H.; Gu, Y.; Zhang, X.; Zhang, G.; Shi, T.; Chen, W. Tim-3 Suppresses the Killing Effect of V γ 9V δ 2 T Cells on Colon Cancer Cells by Reducing Perforin and Granzyme B Expression. *Exp. Cell Res.* **2020**, *386*, 111719. [[CrossRef](#)]
69. Hong, Y.; Zhang, L.; Tian, X.; Xiang, X.; Yu, Y.; Zeng, Z.; Cao, Y.; Chen, S.; Sun, A. Identification of Immune Subtypes of Ph-Neg B-ALL with Ferroptosis Related Genes and the Potential Implementation of Sorafenib. *BMC Cancer* **2021**, *21*, 1331. [[CrossRef](#)]
70. Yadav, B.D.; Samuels, A.L.; Wells, J.E.; Sutton, R.; Venn, N.C.; Bendak, K.; Anderson, D.; Marshall, G.M.; Cole, C.H.; Beesley, A.H.; et al. Heterogeneity in Mechanisms of Emergent Resistance in Pediatric T-Cell Acute Lymphoblastic Leukemia. *Oncotarget* **2016**, *7*, 58728–58742. [[CrossRef](#)]
71. Dufva, O.; Pölönen, P.; Brück, O.; Keränen, M.A.I.; Klievink, J.; Mehtonen, J.; Huuhtanen, J.; Kumar, A.; Malani, D.; Siitonen, S.; et al. Immunogenomic Landscape of Hematological Malignancies. *Cancer Cell* **2020**, *38*, 424–428. [[CrossRef](#)] [[PubMed](#)]
72. Pearce, E.L.; Mullen, A.C.; Martins, G.A.; Krawczyk, C.M.; Hutchins, A.S.; Zediak, V.P.; Banica, M.; DiCioccio, C.B.; Gross, D.A.; Mao, C.; et al. Control of Effector CD8+ T Cell Function by the Transcription Factor Eomesodermin. *Science* **2003**, *302*, 1041–1043. [[CrossRef](#)] [[PubMed](#)]

73. Chen, Z.; Ji, Z.; Ngiow, S.F.; Manne, S.; Cai, Z.; Huang, A.C.; Johnson, J.; Staupé, R.P.; Bengsch, B.; Xu, C.; et al. TCF-1-Centered Transcriptional Network Drives an Effector versus Exhausted CD8 T Cell-Fate Decision. *Immunity* **2019**, *51*, 840–855.e5. [[CrossRef](#)] [[PubMed](#)]
74. Lino, C.N.R.; Barros-Martins, J.; Oberdörfer, L.; Walzer, T.; Prinz, I. Eomes Expression Reports the Progressive Differentiation of IFN- γ -Producing Th1-like $\Gamma\delta$ T Cells. *Eur. J. Immunol.* **2017**, *47*, 970–981. [[CrossRef](#)] [[PubMed](#)]
75. Cheung, L.C.; Tickner, J.; Hughes, A.M.; Skut, P.; Howlett, M.; Foley, B.; Oommen, J.; Wells, J.E.; He, B.; Singh, S.; et al. New Therapeutic Opportunities from Dissecting the Pre-B Leukemia Bone Marrow Microenvironment. *Leukemia* **2018**, *32*, 2326–2338. [[CrossRef](#)] [[PubMed](#)]
76. Bertaina, A.; Zorzoli, A.; Petretto, A.; Barbarito, G.; Inglese, E.; Merli, P.; Lavarello, C.; Brescia, L.P.; De Angelis, B.; Tripodi, G.; et al. Zoledronic Acid Boosts $\Gamma\delta$ T-Cell Activity in Children Receiving A β + T and CD19+ Cell-Depleted Grafts from an HLA-Haplo-Identical Donor. *Oncoimmunology* **2016**, *6*, e1216291. [[CrossRef](#)]
77. Chew, V.; Lai, L.; Pan, L.; Lim, C.J.; Li, J.; Ong, R.; Chua, C.; Leong, J.Y.; Lim, K.H.; Toh, H.C.; et al. Delineation of an Immunosuppressive Gradient in Hepatocellular Carcinoma Using High-Dimensional Proteomic and Transcriptomic Analyses. *Proc. Natl. Acad. Sci. USA* **2017**, *114*, E5900–E5909. [[CrossRef](#)]
78. Xu, B.; Yuan, L.; Gao, Q.; Yuan, P.; Zhao, P.; Yuan, H.; Fan, H.; Li, T.; Qin, P.; Han, L.; et al. Circulating and Tumor-Infiltrating Tim-3 in Patients with Colorectal Cancer. *Oncotarget* **2015**, *6*, 20592–20603. [[CrossRef](#)]
79. Brauneck, F.; Weimer, P.; Schulze Zur Wiesch, J.; Weisel, K.; Leyboldt, L.; Vohwinkel, G.; Fritzsche, B.; Bokemeyer, C.; Wellbrock, J.; Fiedler, W. Bone Marrow-Resident V δ 1 T Cells Co-Express TIGIT With PD-1, TIM-3 or CD39 in AML and Myeloma. *Front. Med. (Lausanne)* **2021**, *8*, 763773. [[CrossRef](#)]
80. De Vries, N.L.; van de Haar, J.; Veninga, V.; Chalabi, M.; Ijsselsteijn, M.E.; van der Ploeg, M.; van den Bulk, J.; Ruano, D.; van den Berg, J.G.; Haanen, J.B.; et al. $\Gamma\delta$ T Cells Are Effectors of Immunotherapy in Cancers with HLA Class I Defects. *Nature* **2023**, *613*, 743–750. [[CrossRef](#)]
81. Koay, H.-F.; Lynch, L. $\Gamma\delta$ T Cells Unveil Invisible Tumors. *Trends Immunol.* **2023**, *44*, 159–161. [[CrossRef](#)] [[PubMed](#)]

Disclaimer/Publisher’s Note: The statements, opinions and data contained in all publications are solely those of the individual author(s) and contributor(s) and not of MDPI and/or the editor(s). MDPI and/or the editor(s) disclaim responsibility for any injury to people or property resulting from any ideas, methods, instructions or products referred to in the content.